ELSEVIER

Physica A 265 (1999) 297–310

PHYSICA A

Jamming transitions and the modified Korteweg–de Vries equation in a two-lane traffic flow

Takashi Nagatani *

Division of Thermal Science, College of Engineering, Shizuoka University, Hamamatsu 432-8561, Japan

Received 23 November 1998

Abstract

The two lattice models are presented to simulate the traffic flow on a two-lane highway. They are the lattice versions of the hydrodynamic model of traffic: the one (model A) is described by the differential-difference equation where time is a continuous variable and space is a discrete variable, and the other (model B) is the difference equation in which both time and space variables are discrete. The jamming transitions among the freely moving phase, the coexisting phase, and the uniform congested phase are studied by using the nonlinear analysis and the computer simulation. The modified Korteweg–de Vries (MKdV) equations are derived from the lattice models near the critical point. The traffic jam is described by a kink–antikink solution obtained from the MKdV equation. It is found that the critical point, the coexisting curve, and the neutral stability line decrease with increasing the rate of lane changing. Also, the computer simulation is performed for the model B. It is shown that the coexisting curves obtained from the MKdV equation are consistent with the simulation result.

PACS: 05.70.Fh; 05.70.jk; 89.40.+k

Keywords: Traffic flow; Phase transition; Critical phenomenon; Modified KdV equation

1. Introduction

Recently, traffic problems have attracted considerable attention [1,2]. A variety of approaches have been applied to describe the collective properties of traffic flow [3–24]. The jamming transitions between the freely moving traffic and the jammed traffic have been found in the traffic models. The transitions have also been observed

* Fax: +81-053-478-1048; e-mail: tmtnaga@eng.shizuoka.ac.jp.

0378-4371/99/$ – see front matter
PII: S0378-4371(98)00563-9

in the actual traffic [25]. The jamming transitions have the properties very similar to the conventional phase transition.

The jamming transitions have been studied by the computer simulation mainly. Very recently, the nonlinear analysis have been performed by a few researchers to investigate the traffic jam. Kurtze and Hong [26] have derived the Korteweg–de Vries (KdV) equation from the hydrodynamic model. They have showed that the traffic soliton appears near the neutral stability line. Komatsu and Sasa [27] have derived the MKdV equation from the car following model. They have showed that the traffic jam is described in terms of a kink–antikink density wave near the critical point. The MKdV equation has been derived from the extended model [28] and the difference equation model [29].

Nagatani [30] has derived the time-dependent Ginzburg–Landau (TDGL) equation from the car following models and has presented the thermodynamic formulation for the jamming transition. It has been shown that the jamming transition in traffic flow is described in terms of thermodynamic terminology of phase transitions and critical phenomena. The freely moving traffic and jammed traffic correspond, respectively, to the gas and liquid phases in the conventional gas–liquid-phase transition: the car density or headway correspond to the density or volume and the sensitivity parameter (the inverse of the delay time) corresponds to temperature. The coexisting curve, the spinodal line and the critical point are obtained by the derivatives of the thermodynamic potential which is derived from the car following models. Also, the TDGL equation can be derived from the MKdV equation with a special perturbed term. Generally, the MKdV equation cannot reduce to the TDGL equation.

Until now, the nonlinear analysis has been applied to the single-lane traffic flow, and the MKdV and TDGL equations have been derived. However, there are little analytical work for the two-lane traffic flow. The two-lane traffic has been studied mainly by the cellular automaton models [31–34]. The hydrodynamic model and the car following model for the two-lane traffic flow are unknown.

In this paper, we present the lattice models of continuum traffic models on a two-lane highway. We study the two-lane traffic flow by using the nonlinear analysis and computer simulation. We derive the MKdV equation for the two-lane traffic flow. We obtain the analytical solution of traffic jams from the MKdV equation. We compare the analytical result with the simulation result.

2. Lattice models

For later convenience, we present the lattice version of the continuum models on a single-lane highway [35]. The model is described by the following differential-difference equations with time lag:

$$\partial_t \rho_j + \rho_0(\rho_j v_j - \rho_{j-1} v_{j-1}) = 0\,, \tag{1}$$

$$\rho_j(t+\tau) v_j(t+\tau) = \rho_0 V(\rho_{j+1}(t))\,, \tag{2}$$

where the subscript j indicates site j on the one-dimensional lattice. $\rho_j(t)$ and $v_j(t)$ represent, respectively, the density and velocity on site j at time t. ρ_0 is the average density. Eq. (1) is the lattice version of continuity equation which relates the local density $\rho_j(t)$ of traffic to the local average speed $v_j(t)$. The space variable is a dimensionless variable divided by the average headway $1/\rho_0$. The lattice spacing is taken to be the average headway $1/\rho_0$. Eq. (2) is the evolution equation in the place of the Navier–Stokes equation. The function $V(\rho)$ is called as the optimal velocity. It is given by

$$V(\rho) = \tanh\left(\frac{1}{\rho} - \frac{1}{\rho_c}\right) + \tanh\left(\frac{1}{\rho_c}\right). \tag{3}$$

This function is the same as that used by Bando et al. [5]. For the symmetry of density, we adopt the following optimal function:

$$V(\rho) = \tanh\left(\frac{2}{\rho_0} - \frac{\rho}{\rho_0^2} - \frac{1}{\rho_c}\right) + \tanh\left(\frac{1}{\rho_c}\right). \tag{4}$$

This function has the turning point (inflection point) at $\rho = \rho_c$, when $\rho_0 = \rho_c$. The delay time τ allows for the time lag that it takes the traffic current to reach the optimal current $\rho_0 V(\rho_{j+1}(t))$ when the traffic flow is varying. The idea is that traffic current $\rho_j(t)v_j(t)$ on site j at time t is adjusted by the optimal current $\rho_0 V(\rho_{j+1}(t-\tau))$ on site $j+1$ at time $t-\tau$. This is similar to the idea of the car following model analyzed by Newell [3] and Whitham [4]. In the above model, we performed the computer simulation and confirmed that the traffic jam occurs within a range of density. Also, we analyzed the above model and derived the MKdV equation from Eqs. (1) and (2) [35].

We extend the single-lane model to the two-lane traffic. Fig. 1 shows the schematic model of traffic flow on a two-lane highway. Let us consider the conservation of car density at site j on the first lane. Without lane changing, the continuity Eq. (1) is obtained from the conservation law of density at site j. We assume that if the density at site $j-1$ on the second lane is higher than that at site j on the first lane, the lane changing occurs from the second lane to the first lane with the following rate: $\gamma|\rho_0^2 V'(\rho_0)|(\rho_{2,j-1}(t) - \rho_{1,j}(t))$ where $\rho_{1,j}(t)$ and $\rho_{2,j}(t)$ are the densities on the first and second lanes. We represent the rate constant coefficient γ to be dimensionless. Constant $|\rho_0^2 V'(\rho_0)|$ is introduced in order to be dimensionless. Similarly, if the density at site j on the first lane is higher than that at site $j+1$ on the second lane, the lane changing occurs from the first lane to the second lane with the rate: $\gamma|\rho_0^2 V'(\rho_0)|(\rho_{1,j}(t) - \rho_{2,j+1}(t))$.

Thus, we obtain the continuity equation on the first lane

$$\partial_t \rho_{1,j} + \rho_0(\rho_{1,j}v_{1,j} - \rho_{1,j-1}v_{1,j-1}) = \gamma|\rho_0^2 V'(\rho_0)|(\rho_{2,j+1} - 2\rho_{1,j} + \rho_{2,j-1}). \tag{5}$$

Similarly, we obtain the continuity equation on the second lane

$$\partial_t \rho_{2,j} + \rho_0(\rho_{2,j}v_{2,j} - \rho_{2,j-1}v_{2,j-1}) = \gamma|\rho_0^2 V'(\rho_0)|(\rho_{1,j+1} - 2\rho_{2,j} + \rho_{1,j-1}). \tag{6}$$

By adding (5) to (6), one obtains the continuity equation for the two-lane traffic

$$\partial_t \rho_j + \rho_0(\rho_j v_j - \rho_{j-1}v_{j-1}) = \gamma|\rho_0^2 V'(\rho_0)|(\rho_{j+1} - 2\rho_j + \rho_{j-1}), \tag{7}$$

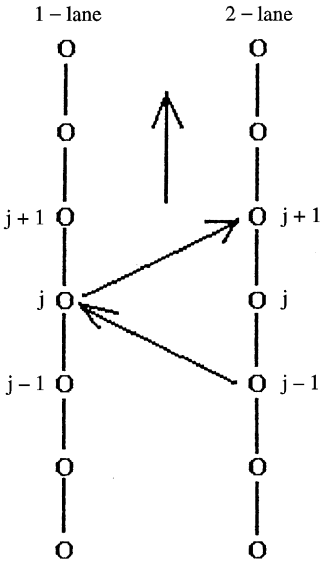

Fig. 1. The schematic model of traffic flow on a two-lane highway. If the density at site $j-1$ on the second lane is higher than that at site j on the first lane, the lane changing occurs from the second lane to the first lane with the rate proportional to the density difference.

where

$$\rho_j = \frac{\rho_{1,j} + \rho_{2,j}}{2} \quad \text{and} \quad \rho_j v_j = \frac{\rho_{1,j} v_{1,j} + \rho_{2,j} v_{2,j}}{2}.$$

We assume that the evolution equation of traffic current on each lane does not change by lane changing. One obtains the evolution equation for the two-lane traffic

$$\rho_j(t+\tau) v_j(t+\tau) = \rho_0 V_e(\rho_{j+1}(t)) , \tag{8}$$

where $V_e(\rho_j) = (V(\rho_{1,j} + V(\rho_{2,j}))/2$. We assume that the optimal velocity function is given by (4). Then, we obtain the governing Eqs. (7) and (8) for the two-lane traffic flow. We call the traffic model by (7) and (8) as model A. Model A is described by the differential-difference equation where time is continuous and space is discrete.

We consider model B in which both space and time are discrete variables. Model B is described by the following equations:

$$\rho_j(t+\tau) - \rho_j(t) + \tau\rho_0[\rho_j(t) v_j(t) - \rho_{j-1}(t) v_{j-1}(t)]$$
$$= \tau\gamma|\rho_0^2 V'(\rho_0)|[\rho_{j+1}(t) - 2\rho_j(t) + \rho_{j-1}(t)] , \tag{9}$$

$$\rho_j(t+\tau) v_j(t+\tau) = \rho_0 V_e(\rho_{j+1}(t)) . \tag{10}$$

By eliminating velocity in Eqs. (7) and (8) (Eqs. (9) and (10)), one obtains the density equations of models A and B:

$$\partial_t \rho_j(t+\tau) + \rho_0^2[V_e(\rho_{j+1}(t)) - V_e(\rho_j(t))]$$
$$-\gamma|\rho_0^2 V'(\rho_0)|[\rho_{j+1}(t+\tau) - 2\rho_j(t+\tau) + \rho_{j-1}(t+\tau)] = 0 , \tag{11}$$

$$\rho_j(t+2\tau)-\rho_j(t+\tau)+\tau\rho_0^2[V_e(\rho_{j+1}(t))-V_e(\rho_j(t))]$$
$$-\tau\gamma|\rho_0^2V'(\rho_0)|[\rho_{j+1}(t+\tau)-2\rho_j(t+\tau)+\rho_{j-1}(t+\tau)]=0\,. \quad (12)$$

The last term on the left side of each equation represents the diffusive behavior induced by the lane changing. It may be expected that the traffic jam is reduced by the diffusive property of the lane changing. Hereafter, we represent $V_e(\rho)$ as $V(\rho)$.

3. Linear stability analysis

We apply the linear stability method to traffic models A and B described by Eqs. (11) and (12). Initially, we consider the stability of the uniform traffic flow. The uniform traffic flow is defined by such a state as a traffic flow with constant density ρ_0 and constant velocity $V(\rho_0)$. The solution of the uniform steady state is given for models A and B

$$\rho_j(t)=\rho_0 \quad \text{and} \quad v_j(t)=V(\rho_0)\,. \quad (13)$$

Let $y_j(t)$ be a small deviation from the uniform steady-state flow: $\rho_j(t)=\rho_0+y_j(t)$. Then, the linearized equations are obtained from (11) and(12)

$$\partial_t y_j(t+\tau)+\rho_0^2V'(\rho_0)[y_{j+1}(t)-y_j(t)]$$
$$-\gamma|\rho_0^2V'(\rho_0)|[y_{j+1}(t+\tau)-2y_j(t+\tau)+y_{j-1}(t+\tau)]=0\,, \quad (14)$$

$$y_j(t+2\tau)-y_j(t+\tau)+\tau\rho_0^2V'(\rho_0)[y_{j+1}(t)-y_j(t)]$$
$$-\tau\gamma|\rho_0^2V'(\rho_0)|[y_{j+1}(t+\tau)-2y_j(t+\tau)+y_{j-1}(t+\tau)]=0\,, \quad (15)$$

where $V'(\rho_0)=\frac{dV_e(\rho)}{d\rho}|_{\rho=\rho_0}$.

By expanding $y_j(t)\propto\exp(ikj+zt)$, the following equations of z are derived, respectively,

$$ze^{z\tau}+\rho_0^2V'(e^{ik}-1)-\gamma|\rho_0^2V'|e^{z\tau}(e^{ik}-2+e^{-ik})=0\,, \quad (16)$$

$$e^{2z\tau}-e^{z\tau}+\tau\rho_0^2V'(e^{ik}-1)-\tau\gamma|\rho_0^2V'|e^{z\tau}(e^{ik}-2+e^{-ik})=0\,, \quad (17)$$

where $V'=V'(\rho_0)$.

By expanding $z=z_1(ik)+z_2(ik)^2+---$, the first- and second-order terms of ik are obtained, respectively, for models A and B

$$z_1=-\rho_0^2V' \quad \text{and} \quad z_2=-\tau(\rho_0^2V')^2-\frac{(1+2\gamma)}{2}\rho_0^2V'\,, \quad (18)$$

$$z_1=-\rho_0^2V' \quad \text{and} \quad z_2=-\frac{3}{2}\tau(\rho_0^2V')^2-\frac{(1+2\gamma)}{2}\rho_0^2V'\,. \quad (19)$$

If z_2 is a negative value, the uniform steady-state flow becomes unstable for long wavelength modes. When z_2 is a positive value, the uniform flow is stable. The neutral

stability conditions are given, respectively, for models A and B

$$\tau = -\frac{(1+2\gamma)}{2\rho_0^2 V'}\,, \tag{20}$$

$$\tau = -\frac{(1+2\gamma)}{3\rho_0^2 V'}\,. \tag{21}$$

For small disturbances with long wavelengths, the uniform traffic flow is unstable if

$$\tau > -\frac{(1+2\gamma)}{2\rho_0^2 V'} \quad \text{for model A}\,, \tag{22}$$

$$\tau > -\frac{(1+2\gamma)}{3\rho_0^2 V'} \quad \text{for model B}\,. \tag{23}$$

The derivative $V'(\rho_0)$ of optimal velocity has the minimal value at turning point $\rho_0 = \rho_c$. Therefore, if $\tau < \tau_c$ ($\tau_c = -(1+2\gamma)/2\rho_0^2 V' = (1+2\gamma)/2$ for model A and $\tau_c = -(1+2\gamma)/3\rho_0^2 V' = (1+2\gamma)/3$ for model B), the uniform flow is always stable irrespective of density. We find that there is a critical point at $\rho = \rho_c$ and $\tau = \tau_c$. When $\gamma = 0$, the critical points and the neutral stability curves are consistent with those in a single-lane traffic flow [35]. With increasing the lane changing rate (with the increase of γ), the critical points and the neutral stability curves decrease. The lane changing stabilizes the uniform traffic flow. The traffic jam is reduced by the lane changing.

4. Nonlinear analysis

We now consider long wavelength modes in traffic flow on coarse-grained scales. The simplest way to describe the long wavelength modes is the long-wave expansion. We consider the slowly varying behavior at long wavelengths near the critical point (ρ_c, τ_c). We extract slow scales for space variable j and time variable t [36]. For $0 < \varepsilon \ll 1$, we therefore define the slow variables X and T:

$$X = \varepsilon(j + bt) \quad \text{and} \quad T = \varepsilon^3 t\,, \tag{24}$$

where b is a constant determined later. We set the density as

$$\rho_j(t) = \rho_c + \varepsilon R(X, T)\,. \tag{25}$$

By expanding Eqs. (11) and (12) to the fifth order of ε with the use of (24) and (25), one obtains the following nonlinear partial differential equations for models A and B:

$$\begin{aligned}
&\varepsilon^2(b + \rho_c^2 V')\partial_X R + \varepsilon^3\left[b^2\tau + \frac{(1+2\gamma)}{2}\rho_c^2 V'\right]\partial_X^2 R \\
&+\varepsilon^4\left[\partial_T R + \left(\frac{b^3\tau^2}{2} + \frac{\rho_c^2 V'}{6} + \gamma\rho_c^2 V' b\tau\right)\partial_X^3 R + \frac{\rho_c^2 V'''}{6}\partial_X R^3\right] + \varepsilon^5\left[2b\,\tau\partial_X\partial_T R\right. \\
&\left. + \left(\frac{b^4\tau^3}{6} + \frac{\rho_c^2 V'}{24} + \frac{\gamma\rho_c^2 V'(b\tau)^2}{2} + \frac{\gamma\rho_c^2 V'}{12}\right)\partial_X^4 R + \frac{\rho_c^2 V'''}{12}\partial_X^2 R^3\right] = 0\,,
\end{aligned} \tag{26}$$

$$\varepsilon^2(b+\rho_c^2V')\partial_X R+\varepsilon^3\left[\frac{3b^2\tau}{2}+\frac{(1+2\gamma)}{2}\rho_c^2V'\right]\partial_X^2 R$$

$$+\varepsilon^4\left[\partial_T R+\left(\frac{7b^3\tau^2}{6}+\frac{\rho_c^2V'}{6}+\gamma\rho_c^2V'b\tau\right)\partial_X^3 R+\frac{\rho_c^2V'''}{6}\partial_X R^3\right]+\varepsilon^5\left[3b\tau\partial_X\partial_T R\right.$$

$$\left.+\left(\frac{5b^4\tau^3}{8}+\frac{\rho_c^2V'}{24}+\frac{\gamma\rho_c^2V'(b\tau)^2}{2}+\frac{\gamma\rho_c^2V'}{12}\right)\partial_X^4 R+\frac{\rho_c^2V'''}{12}\partial_X^2 R^3\right]=0\,, \quad (27)$$

where

$$V'=\left.\frac{dV(\rho)}{d\rho}\right|_{\rho=\rho_c} \quad \text{and} \quad V'''=\left.\frac{d^3V(\rho)}{d\rho^3}\right|_{\rho=\rho_c}.$$

Here we used the expansions shown in the appendix.

By taking $b=-\rho_c^2V'(\rho_c)$, the second-order terms of ε are eliminated from Eqs. (26) and (27). We consider the neighborhood of the critical point τ_c:

$$\frac{\tau}{\tau_c}=1+\varepsilon^2\,, \quad (28)$$

where

$$\tau_c=-\frac{(1+2\gamma)}{2\rho_0^2V'}=\frac{1+2\gamma}{2}$$

for model A and $\tau_c=-\frac{(1+2\gamma)}{3\rho_0^2V'}=\frac{1+2\gamma}{3}$ for model B. Eqs. (26) and (27) are written

$$\varepsilon^4\left[\partial_T R-\frac{(1+12\gamma^2)}{24}(-\rho_c^2V')\partial_X^3 R+\frac{\rho_c^2V'''}{6}\partial_X R^3\right]$$

$$+\varepsilon^5\left[\frac{(1+2\gamma)}{2}(-\rho_c^2V')\partial_X^2 R+\frac{(1+12\gamma^2+32\gamma^3)}{48}(-\rho_c^2V')\partial_X^4 R\right.$$

$$\left.-\frac{(1+4\gamma)}{12}\rho_c^2V'''\partial_X^2 R^3\right]=0\,, \quad (29)$$

$$\varepsilon^4\left[\partial_T R-\frac{(1-5\gamma+4\gamma^2)}{27}(-\rho_c^2V')\partial_X^3 R+\frac{\rho_c^2V'''}{6}\partial_X R^3\right]$$

$$+\varepsilon^5\left[\frac{(1+2\gamma)}{2}(-\rho_c^2V')\partial_X^2 R+\frac{(1-6\gamma-9\gamma^2+14\gamma^3)}{54}(-\rho_c^2V')\partial_X^4 R\right.$$

$$\left.-\frac{(1+4\gamma)}{12}\rho_c^2V'''\partial_X^2 R^3\right]=0\,. \quad (30)$$

In order to derive the regularized equation, we make the following transformations for (29) and (30):

$$T'=\frac{(1+12\gamma^2)(-\rho_c^2V')}{24}T \quad \text{and} \quad R=\left(\frac{-(1+12\gamma^2)\rho_c^2V'}{4\rho_c^2V'''}\right)^{1/2}R'\,, \quad (31)$$

$$T' = \frac{(1-5\gamma+4\gamma^2)(-\rho_c^2 V')}{27} T \quad \text{and} \quad R = \left(\frac{-2(1-5\gamma+4\gamma^2)\rho_c^2 V'}{9\rho_c^2 V'''} \right)^{1/2} R' . \tag{32}$$

One obtains the regularized equations for models A and B

$$\partial_{T'} R' = \partial_X^3 R' - \partial_X R'^3 - \varepsilon \left[\frac{12(1+2\gamma)}{(1+12\gamma^2)} \partial_X^2 R' + \frac{(1+12\gamma^2+32\gamma^3)}{2(1+12\gamma^2)} \partial_X^4 R' - \frac{(1+4\gamma)}{2} \partial_X^2 R'^3 \right], \tag{33}$$

$$\partial_{T'} R' = \partial_X^3 R' - \partial_X R'^3 - \varepsilon \left[\frac{27(1+2\gamma)}{2(1-5\gamma+4\gamma^2)} \partial_X^2 R' + \frac{(1-6\gamma-9\gamma^2+14\gamma^3)}{2(1-5\gamma+4\gamma^2)} \partial_X^4 R' - \frac{(1+4\gamma)}{2} \partial_X^2 R'^3 \right]. \tag{34}$$

If we ignore the O(ε) terms in Eqs. (33) and (34), they are just the MKdV equations with a kink solution as the desired solution

$$R'_0(X,T') = \sqrt{c}\, \tanh \sqrt{\frac{c}{2}} (X - cT') . \tag{35}$$

Next, assuming that $R'(X,T') = R'_0(X,T') + \varepsilon R'_1(X,T')$, we take into account the O(ε) correction. In order to determine the selected value of the propagation velocity c for the kink solution (35), it is necessary to satisfy the solvability condition

$$(R'_0, M[R'_0]) \equiv \int_{-\infty}^{+\infty} dX\, R'_0\, M[R'_0] = 0 , \tag{36}$$

where

$$M[R'_0] = \frac{12(1+2\gamma)}{(1+12\gamma^2)} \partial_X^2 R' + \frac{(1+12\gamma^2+32\gamma^3)}{2(1+12\gamma^2)} \partial_X^4 R' - \frac{(1+4\gamma)}{2} \partial_X^2 R'^3$$

for (33) and

$$M[R'_0] = \frac{27(1+2\gamma)}{2(1-5\gamma+4\gamma^2)} \partial_X^2 R' + \frac{(1-6\gamma-9\gamma^2+14\gamma^3)}{2(1-5\gamma+4\gamma^2)} \partial_X^4 R' - \frac{(1+4\gamma)}{2} \partial_X^2 R'^3$$

for (34).

By performing the integration, we obtain the selected velocities

$$c = \frac{120(1+2\gamma)}{(5+12\gamma+24\gamma^2+64\gamma^3)} \quad \text{for (33)} , \tag{37}$$

$$c = \frac{135(1+2\gamma)}{(5-15\gamma-66\gamma^2+76\gamma^3)} \quad \text{for (34)} . \tag{38}$$

One obtains the solutions for models A and B

$$R(X,T) = \sqrt{\frac{(1+12\gamma^2)c(-\rho_c^2 V')}{4\rho_c^2 V'''}} \times \tanh \sqrt{\frac{c}{2}} \left(X - \frac{(1+12\gamma^2)c(-\rho_c^2 V')}{24} T \right) \quad \text{with (37)} , \tag{39}$$

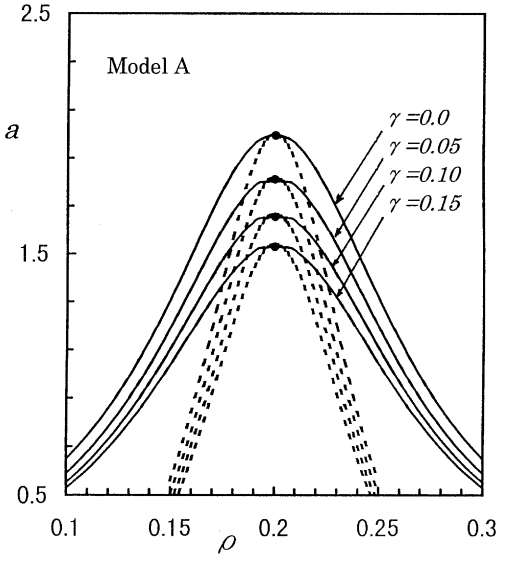

Fig. 2. The phase diagram on (ρ, a)-plane for model A. The critical points are indicated by the full circles. The solid curves and the dotted lines indicate the coexisting curves (phase separation lines) and the neutral stability lines for $\gamma = 0.0, 0.05, 0.10,$ and 0.15.

$$R(X,T) = \sqrt{\frac{2(1-5\gamma+4\gamma^2)c(-\rho_c^2 V')}{9\rho_c^2 V'''}} \times \tanh\sqrt{\frac{c}{2}}\left(X - \frac{(1-5\gamma+4\gamma^2)c(-\rho_c^2 V')}{27}T\right) \quad \text{with (38)}. \tag{40}$$

If we adopt the explicit form (4) of the optimal velocity ($-\rho_c^2 V' = 1,\ \rho_c^6 V''' = 2$), the amplitude A of the kink solutions are given, respectively, for models A and B

$$A = \rho_c^2\sqrt{\frac{15(1+12\gamma^2)(1+2\gamma)}{(5+12\gamma+24\gamma^2+64\gamma^3)}\left(\frac{a_c}{a}-1\right)} \quad \text{with} \quad a_c = \tau_c^{-1} = \frac{2}{1+2\gamma}, \tag{41}$$

$$A = \rho_c^2\sqrt{\frac{15(1-5\gamma+4\gamma^2)(1+2\gamma)}{(5-15\gamma-66\gamma^2+76\gamma^3)}\left(\frac{a_c}{a}-1\right)} \quad \text{with} \quad a_c = \tau_c^{-1} = \frac{3}{1+2\gamma}. \tag{42}$$

The kink solution represents the coexisting phase which consists of the freely moving phase with low density and the jammed (or congested) phase with high density. The densities of the freely moving phase and the congested phase are given, respectively, by $\rho = \rho_c - A$ and $\rho = \rho_c + A$. Thus, we obtain the phase diagram in the (ρ, a)-plane where ρ is the density and a is the sensitivity (the inverse of delay time τ). Figs. 2 and 3 show the coexisting curves together with the neutral stability lines, respectively, for models A and B. The solid curves and the dotted lines indicate, respectively, the coexisting

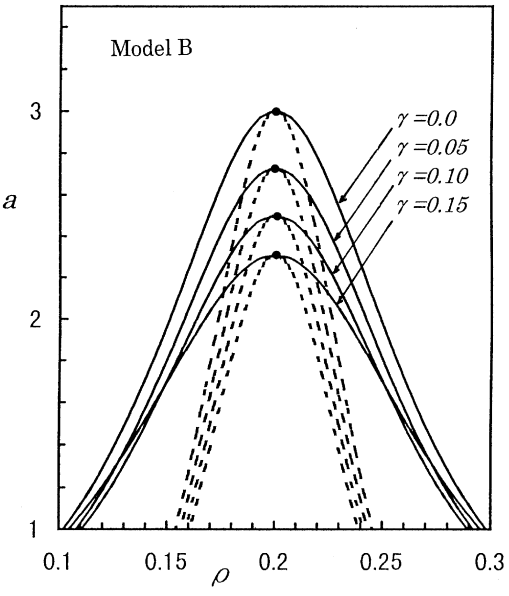

Fig. 3. The phase diagram on (ρ, a)-plane for model B. The critical points are indicated by the full circles. The solid curves and the dotted lines indicate the coexisting curves (phase separation lines) and the neutral stability lines for $\gamma = 0.0, 0.05, 0.10$, and 0.15.

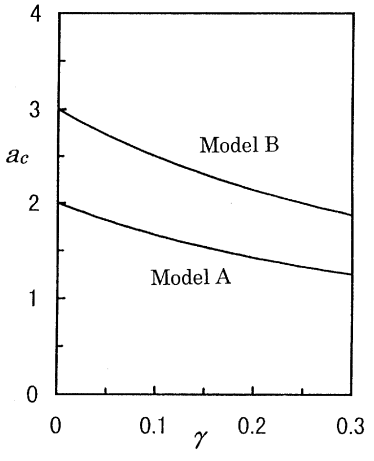

Fig. 4. The plot of critical point a_c against rate γ of lane changing.

curves and the neutral stability lines. Fig. 4 shows the dependence of critical point a_c upon rate γ of lane changing. The limit of $\gamma = 0$ represents the coexisting and neutral stability curves of the single-lane traffic flow. With increasing rate γ of the lane changing, the critical point, the coexisting curve and the neutral stability line decrease.

The lane changing stabilizes the uniform traffic. The occurrence of traffic jam is reduced to the low value of the sensitivity. Therefore, the lane changing has an important effect on the stability of the uniform traffic.

5. Simulation

We carry out simulation to derive numerically the phase separation lines (coexisting curves) and to compare the simulation result with the analytical result. We perform the computer simulation for model B since it is easier to perform a numerical simulation of model B than model A. A priori it could not be assumed that model B would yield similar traffic patterns to the single-lane traffic flow. Therefore, simulation is carried out to validate two points. (1) First it has to be shown that model B is indeed capable of describing traffic dynamics. (2) Next the applicability of the nonlinear analysis has to be proven.

We set τ as the unit time step. One obtains from (12) the following:

$$\rho_j(t+2)-\rho_j(t+1)+\tau\rho_0^2[V_e(\rho_{j+1}(t))-V_e(\rho_j(t))]$$
$$-\tau\gamma|\rho_0^2V'(\rho_0)|[\rho_{j+1}(t+1)-2\rho_j(t+1)+\rho_{j-1}(t+1)]=0. \quad (43)$$

Initially, the density is assumed to be the step function at the average density on the one-dimensional lattice. The boundary is periodic. Traffic patterns are studied at various densities and delay times for small values of γ ($0\leqslant\gamma<0.25$). As a result, three types of traffic flow have to be distinguished: (1) a freely moving phase, (2) a coexisting phase in which jams appear, and (3) a uniform congested phase. The patterns for the coexisting phase are shown in Fig. 5. The patterns (a) and (b) indicate, respectively, the plots of density ρ against space j for $\gamma=0$ and 0.05 where $a=2.5$ and $\rho_c=0.2$. The region with high density represents the traffic jam. The jam propagates from right to left where cars move from left to right. The density wave representing jam propagates with the symmetric kink–antikink form. The strength of the density wave (jam) in pattern (b) is lower than that in pattern (a). In any case considering long-time evolution, only two distinct densities survive for the coexisting phase depending on the delay time and the rate of lane changing. They are the densities of the phase transition points on the coexisting curve. Thus, for each delay time they are calculated from simulation. Fig. 6 shows the densities of the transition points on the coexisting λ curves for $\gamma=0.0, 0.05, 0.10$, and 0.15. The circular, triangular, square, and diamond points indicate, respectively, the simulation data of densities for $\gamma=0.0, 0.05, 0.10$, and 0.15. The solid curves indicate the coexisting curves obtained from the nonlinear analysis. The simulation results agree with the analytical results for small values of γ. However, the transition points of simulation are not consistent with the analytical result for larger value of γ.

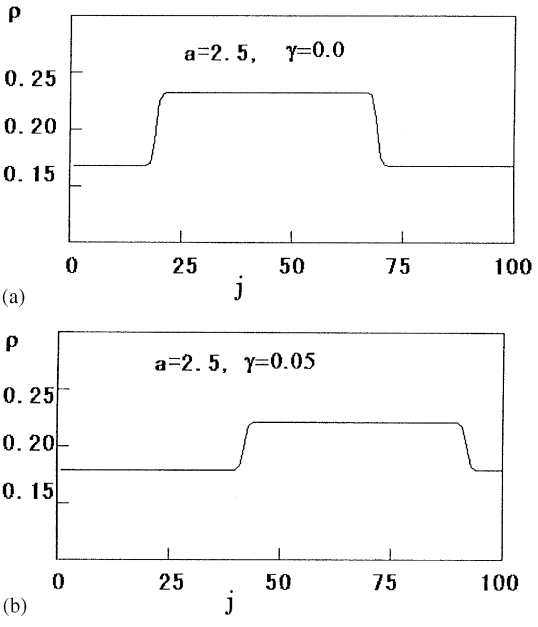

Fig. 5. The patterns for coexisting phase where $a = 2.5$ and $\rho = \rho_c = 0.2$. (a) The plot of density ρ against space j for $\gamma = 0.0$. (b) The plot of density ρ against space j for $\gamma = 0.05$. The region with high density represents the traffic jam.

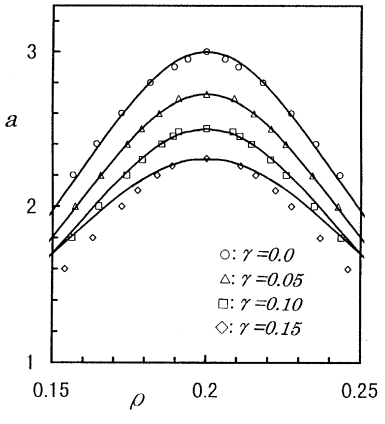

Fig. 6. Phase separation curves (coexisting curves). The circular, triangular, square, and diamond points indicate, respectively, the simulation results for $\gamma = 0.0, 0.05, 0.10$, and 0.15. The solid curves represent the analytical results obtained by the MKdV equation.

6. Summary

We proposed the lattice hydrodynamic models of traffic flow on a two-lane highway. We investigated the traffic behavior analytically by the use of the linear stability theory and the nonlinear wave analysis. We showed that there is a critical point above

which no jam occur for each rate of lane changing. A phase transition occurs among the freely moving phase, the coexisting phase, and the uniform congested phase. We derived the MKdV equation to describe the traffic jam near the critical point. We also performed a numerical simulation for the difference equation model. We obtained the phase diagram and compared the analytical result with the simulation result. The analytical and simulation results near the critical point are in good agreement. We found that the critical point, the coexisting curve, and the neutral stability line decrease with increasing rate of lane changing.

Appendix A

In this appendix, we give the expansions of each term in Eqs. (11) and (12) to fifth-order of ε.

$$\rho_j(t+\tau) = \rho_c + \varepsilon R + \varepsilon^2 b\tau \partial_X R + \varepsilon^3 \frac{(b\tau)^2}{2}\partial_X^2 R + \varepsilon^4 \frac{(b\tau)^3}{6}\partial_X^3 R + \varepsilon^4 \tau \partial_T R + \varepsilon^5 \frac{(b\tau)^4}{24}\partial_X^4 R + \varepsilon^5 b\tau^2 \partial_T \partial_X R\,, \tag{A.1}$$

$$\partial_t \rho_j(t+\tau) = \varepsilon^2 b \partial_X R + \varepsilon^3 b^2 \tau \partial_X^2 R + \varepsilon^4 \frac{b^3\tau^2}{2}\partial_X^3 R + \varepsilon^4 \partial_T R + \varepsilon^5 \frac{b^4\tau^3}{6}\partial_X^4 R + \varepsilon^5 2b\tau \partial_T \partial_X R\,, \tag{A.2}$$

$$\rho_{j+1}(t) = \rho_c + \varepsilon R + \varepsilon^2 \partial_X R + \frac{\varepsilon^3}{2}\partial_X^2 R + \frac{\varepsilon^4}{6}\partial_X^3 R + \frac{\varepsilon^5}{24}\partial_X^4 R\,. \tag{A.3}$$

We expand the optimal velocity function at the turning point:

$$V(\rho_j) = V(\rho_c) + V'(\rho_c)(\rho_j - \rho_c) + \frac{V'''(\rho_c)}{6}(\rho_j - \rho_c)^3\,, \tag{A.4}$$

$$V(\rho_{j+1}) = V(\rho_c) + V'(\rho_c)(\rho_{j+1} - \rho_c) + \frac{V'''(\rho_c)}{6}(\rho_{j+1} - \rho_c)^3\,, \tag{A.5}$$

$$V(\rho_{j+1}) - V(\rho_j) = V'(\rho_c)\left[\varepsilon^2 \partial_X R + \frac{\varepsilon^3}{2}\partial_X^2 R + \frac{\varepsilon^4}{6}\partial_X^3 R + \frac{\varepsilon^5}{24}\partial_X^4 R\right] + \frac{V'''(\rho_c)}{6}\left[\varepsilon^4 \partial_X R^3 + \varepsilon^5 \frac{1}{2}\partial_X^2 R^3\right]. \tag{A.6}$$

By inserting (A.2) and (A.6) into Eq. (11), one obtains Eq. (26).

Also, the following expansion is obtained from (A.1):

$$\rho_j(t+2\tau) = \rho_c + \varepsilon R + \varepsilon^2 2b\tau \partial_X R + \varepsilon^3 \frac{(2b\tau)^2}{2}\partial_X^2 R + \varepsilon^4 \frac{(2b\tau)^3}{6}\partial_X^3 R + \varepsilon^4 2\tau \partial_T R + \varepsilon^5 \frac{(2b\tau)^4}{24}\partial_X^4 R + \varepsilon^5 4b\tau^2 \partial_T \partial_X R\,. \tag{A.7}$$

By inserting (A.1), (A.7) and (A.6) into Eq. (12), one obtains Eq. (27).

References

[1] D.E. Wolf, M. Schreckenberg, A. Bachem (Eds.), Traffic and Granular Flow, World Scientific, Singapore, 1996.
[2] D. Helbing, Verkehrsdynamik, Springer, Berlin, 1997.
[3] G.F. Newell, Oper. Res. 9 (1961) 209.
[4] G.B. Whitham, Proc. Roy. Soc. London A 428 (1990) 49.
[5] M. Bando, K. Hasebe, A. Nakayama, A. Shibata, Y. Sugiyama, Phys. Rev. E 51 (1995) 1035.
[6] K. Nagel, M. Schreckenberg, J. Phys. I 2 (1992) 2221.
[7] M. Schreckenberg, A. Schadschneider, K. Nagel, N. Ito, Phys. Rev. E 51 (1995) 2329.
[8] G. Csanyi, J. Kertestz, J. Phys. A 28 (1995) 427.
[9] S.C. Benjamin, N.F. Johnson, P.M. Hui, J. Phys. A 29 (1996) 3119.
[10] A. Schadschneider, M. Schreckenberg, Ann. Phys. 6 (1997) 541.
[11] O. Biham, A.A. Middleton, D.A. Levine, Phys. Rev. A 46 (1992) R6124.
[12] T. Nagatani, Phys. Rev. E 48 (1993) 3290.
[13] J.A. Cuesta, F.C. Matinez, J.M. Nolera, A. Sanchez, Phys. Rev. E 48 (1993) 4175.
[14] K.H. Chung, P.M. Hui, G.Q. Gu, Phys. Rev. E 51 (1995) 772.
[15] E. Ben-Naim, P.L. Krapivsky, S. Redner, Phys. Rev. E 50 (1994) 822.
[16] T. Nagatani, Phys. Rev. E 51 (1995) 922.
[17] I. Prigogine, R. Herman, Kinetic Theory of Vehicular Traffic, Elsevier, New York, 1971.
[18] S.L. Paveri-Fontana, Transportation Res. 9 (1975) 225.
[19] D. Helbing, Phys. Rev. E 53 (1996) 2366.
[20] D. Helbing, Physica A 233 (1996) 253.
[21] T. Nagatani, Physica A 237 (1997) 67.
[22] B.S. Kerner, P. Konhauser, Phys. Rev. E 48 (1993) 2335.
[23] B.S. Kerner, P. Konhauser, M. Schilke, Phys. Rev. E 51 (1995) 6243.
[24] S. Krauss, P. Wagner, C. Gawron, Phys. Rev. E 55 (1997) 5597.
[25] B.S. Kerner, H. Rehborn, Phys. Rev. E 53 (1996) R1297.
[26] D.A. Kurtze, D.C. Hong, Phys. Rev. E 52 (1995) 218.
[27] T. Komatsu, S. Sasa, Phys. Rev. E 52 (1995) 5574.
[28] T. Nagatani, K. Nakanishi, Phys. Rev. E 57 (1998) 6415.
[29] T. Nagatani, K. Nakanishi, H. Emmerich, J. Phys. A 31 (1998) 5431.
[30] T. Nagatani, Phys. Rev. E 58 (1998) 4271.
[31] T. Nagatani, J. Phys. A 26 (1993) L781.
[32] T. Nagatani, Physica A 202 (1994) 449.
[33] A. Awazu, J. Phys. Soc. Jpn. 67 (1998) 1071.
[34] K. Nagel, D.E. Wolf, P. Wagner, P. Simon, Phys. Rev. E 58 (1998) 1425.
[35] T. Nagatani, Physica A 264 (1999) 581.
[36] M.C. Cross, P.C. Hohenberg, Rev. Mod. Phys. 65 (1993) 851.